Sensors and Actuators B 242 (2017) 673–678

Contents lists available at ScienceDirect

Sensors and Actuators B: Chemical

journal homepage: www.elsevier.com/locate/snb

A fiber ring cavity laser sensor for refractive index and temperature measurement with core-offset modal interferometer as tunable filter

Lu Cai [a], Yong Zhao [a,b,*], Xue-gang Li [a]

[a] College of Information Science and Engineering, Northeastern University, Shenyang 110819, China
[b] State Key Laboratory of Synthetical Automation for Process Industries (Northeastern University), Shenyang 110819, China

ARTICLE INFO

Article history:
Received 11 March 2016
Received in revised form
19 November 2016
Accepted 22 November 2016
Available online 23 November 2016

Keywords:
EDF ring cavity laser
Core-offset joints
MZ interferometer
Temperature measurement
RI measurement

ABSTRACT

In this paper, a fiber ring cavity laser refractive index (RI) and temperature sensor is presented. A core-offset Mach-Zehnder (MZ) interferometer is utilized as a sensing element as well as a filter. The core-offset distances of these two joints fabricated by a common fusion splicer are about 3.7 μm, which well ensure the robustness and tensile strength. The directions of these two offsets are unnecessary to be controlled since low fringe visibility is acceptable in this sensor. The Erbium doped fiber (EDF) ring cavity laser setup is helpful to improve the spectral quality factor Q and the detection limit (DL). The Q value of this laser sensor can be higher than that of ordinary core-offset sensing structures by two magnitudes. By combining the core-offset MZ interferometer with EDF ring cavity laser, the final calculated detection limits for temperature and RI measurement are 0.35 °C and 4.54×10^{-4}, which are 10 times higher than those of the individual MZ interferometer. The proposed sensor possesses the advantages of low cost, simple operation and easy fabrication process.

1. Introduction

Tunable Erbium doped fiber (EDF) ring cavity laser has been researched comprehensively in recent decades. EDF has high laser gain around 1550 nm so it is potential for fiber optics communication and sensing. One of the most common principles is to change the band-pass wavelength of filter through a tailorable filtering structure. The candidate structures include fiber Bragg grating (FBG) [1], long period grating (LPG) [2], Fabry-Perot (FP) cavity [3] and so on. The tuning range of laser wavelength is usually dozens of nanometers. It means that the laser line will move along the adjustment of filter. Thus, it can be used as a sensor to sense those environmental conditions which can change the spectral characteristics in turn [4–6]. A typical system of ring cavity laser sensor is shown as Fig. 1. Pump source is injected into gain medium like Er^{3+} and Yb^{3+} doped optical fiber and then stimulated emission occurs. After recycling in the ring cavity, fluorescence spectrum is recorded by optical spectrum analyzer (OSA). When the sensing structure, such as a FP cavity, is embedded into the EDF ring cavity laser device as sensing part, the comb-shaped interference spectrum acts as a wavelength selector and only one peak is amplified to become the laser line. Furthermore, the spectrum of FP interferometer shifts with the variation of temperature, strain and some other external parameters and it finally results in the shift of the laser wavelength. The linear relationship between the laser wavelength shift and external variation can be calculated as calibration of the laser sensor.

The key merits of the fiber ring cavity laser sensor are narrow full width half maximum (FWHM), high signal-to-noise radio (SNR) and high evanescent radio (ER). Hence, researchers recently come up with combining the EDF ring cavity laser and in-fiber Mach-Zehnder (MZ) interferometer together to construct an in-fiber MZ based fiber ring cavity laser sensor [7–9]. The in-fiber MZ interferometer possesses the advantages of low cost, flexible structure and simple operation. One of the typical structures is core-offset joint which could be cascaded to another core-offset joint [10] or taper [11,12] or multimode fiber (MMF)/thin-core fiber (TCF) [13,14] section and so on. However, sometimes, especially for the shallow taper and the short distance core-offset joint, the quality of interference spectrum is not high and the multiple dips and peaks increase the difficulty of detection. Previously we did some research in core-offset joint pairs for RI sensing and increased RI sensitivity by tapering the middle part [15]. And then it is found that the shortcomings of in-fiber MZ interferometer could be exactly compensated via being embedded into fiber ring cavity laser as a

* Corresponding author at: College of Information Science and Engineering, Northeastern University, Shenyang 110819, China.
E-mail addresses: zhaoyong@ise.neu.edu.cn, zhaoyong@tsinghua.org.cn (Y. Zhao).

http://dx.doi.org/10.1016/j.snb.2016.11.112
0925-4005/

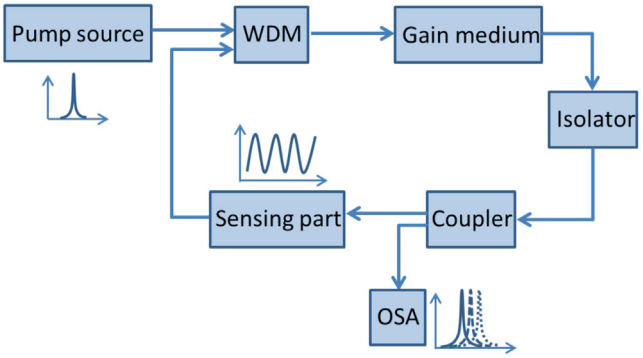

Fig. 1. The schematic diagram of a typical ring cavity laser sensor.

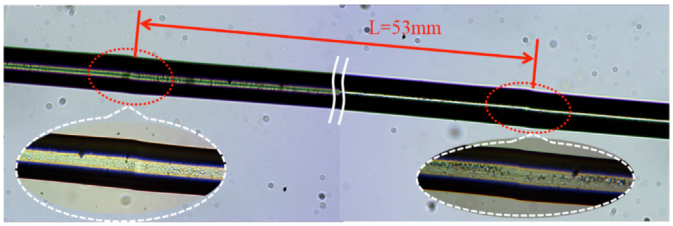

Fig. 2. Micrographs of two core-offset joints.

tunable filter. This kind of resultant sensor makes a complementation to both their advantages and disadvantages. Compared to that previous work and other high-sensitivity in-fiber modal interferometers [16,17], this method jumps out of the trap of remoulding the sensing part. It is no longer to focus on how to design the sensing part finely for high sensitivity but give a consideration to increase the spectrum quality. It improves the sensing performance using simple elements on the premise of guaranteeing the mechanical strength.

In this paper, an EDF ring cavity laser sensor has been investigated. A core-offset Mach-Zehnder (MZ) interferometer is utilized and it has double identities: a sensing element as well as a filter. Two short-distance offsets are easily fabricated through the function of manual welding in a common fusion splicer. And then the interference spectrum of the MZ acts as the pass-band filter of the EDF ring cavity laser. The spectral quality represented by the quality factor Q has been increased significantly. Regarding the improvement of sensing property, the calculation method presented by White I. M. in 2008 [18], which is adopted by many papers, is employed for calculating the sensing detection limit (DL) in this paper. The liquid refractive index (RI) and temperature are tested as measurands in experiment.

2. Sensor setup and principle

The sensor is composed of two core-offset joints of which the micrograph is given in Fig. 2. When the broadband light is injected into the first offset joint, due to the mode field mismatch, part of the light leaks out of fundamental mode and multiple cladding modes are excited. Subsequently, the core and cladding modes propagate in the middle part of SMF simultaneously. The RI difference between fiber core and cladding leads to the phase difference between core and cladding modes. Thus, when these modes arrive at the second offset joint, part of the light loses and the other meets in the SMF core. As a consequence, modal interference occurs between core and cladding modes. Two core-offset joints just play the role as beam splitter and combiner. The SMF used to fabricate the sensor is Corning SMF-28, whose core diameter and cladding diameter are respectively 8.2 μm and 125 μm. Two short

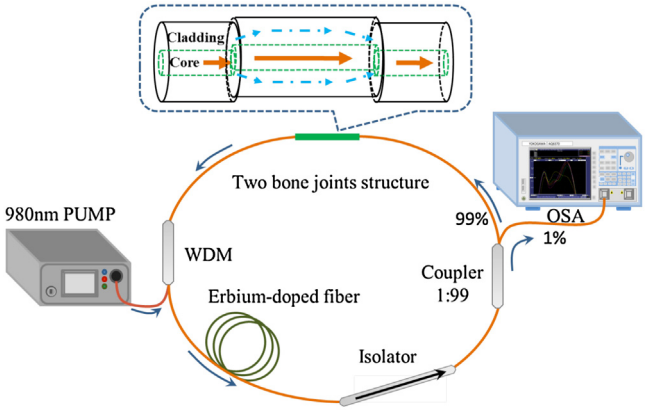

Fig. 3. The schematic diagram of the EDF laser cavity sensor setup.

distance core-offset joints are fabricated apart 53 mm for guarantee of enough fringes.

In the cascaded core-offset joints structure, the offset distance and direction are all important factors to produce high-quality interference spectrum [19]. However, it needs precise translation stage and complex operation. In addition, the large core-offset distance leads to low mechanical strength even though it is helpful to obtain high ER and sensitivity. The large core-offset sensor structure is fragile and easily broken. So as to avoid these problems, the EDF ring cavity laser device is utilized. The core-offset distances in this work are all about 3.7 μm and the directions of these two offsets are unnecessary to be controlled.

The experimental setup for liquid RI and temperature sensing is shown in Fig. 3. Here, a power-tunable laser module with central peak at 974 nm is used as pump source. A wavelength division multiplexer (WDM) for 1550 nm and 980 nm is used to combine and divide the light with different wavelength. It is worth mentioning that the WDM used in experiment is not taper type but filter type. One of the differences between them is the position of three ports. For the filter type WDM, 980 nm port is at the same side with the common port and the 1550 nm port at the other side. A segment of low doped erbium-doped fiber (EDF, Sumitomo) is used as an active medium. Moreover, an optical isolator is inserted into the cavity to ensure unidirectional propagation. A coupler with 1:99 splits the light in two beams and one percentage of the light is launched into the OSA (YOKOGAWA-AQ6370). Via adjusting the pump source at a low-power position, the amplified spontaneous emission (ASE) spectrum of the EDF ring cavity laser device is obtained. And the MZ interference spectrum is given in Fig. 4 in red line. The ERs of these spectra are about 2 dB. The primary reason of the low ER is the large disparity of intensity between core and cladding modes which is caused by the short distance of the offsets. Once the pump power is increased to be high enough, the simulated radiation of EDF would happen. The MZ interference spectrum is a wavelength selector and the pass band with highest intensity (around 1570 nm) is amplified to form a single emission as the green line whose FWHM is measured to be about 0.016 nm. The contribution of the laser system is to narrow the FWHM and increase the ER and SNR. Thus, the spectral quality and the DL of the sensor device are improved.

The DL reports the smallest measurand change that can be accurately measured using this sensor. The DL for measurement is given as:

$$DL = \frac{R}{S} \tag{1}$$

Where S is the measurement sensitivity and R is sensor resolution. According to reference [18], sensor resolution is mainly determined by three factors $\sigma_{ampl-noise}$, $\sigma_{temp-induced}$ and $\sigma_{spect-tes}$ which respec-

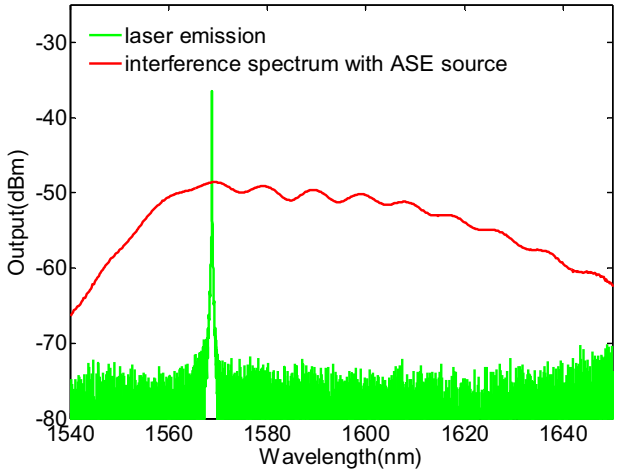

Fig. 4. Transmission spectra for the system with element by low pump power (red line), and with element by high pump power (green line). (For interpretation of the references to colour in this figure legend, the reader is referred to the web version of this article.)

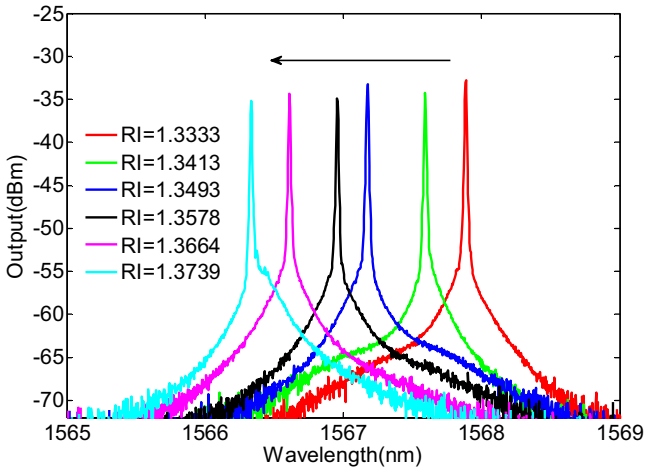

Fig. 5. Measured emission laser lines shifted along different RI.

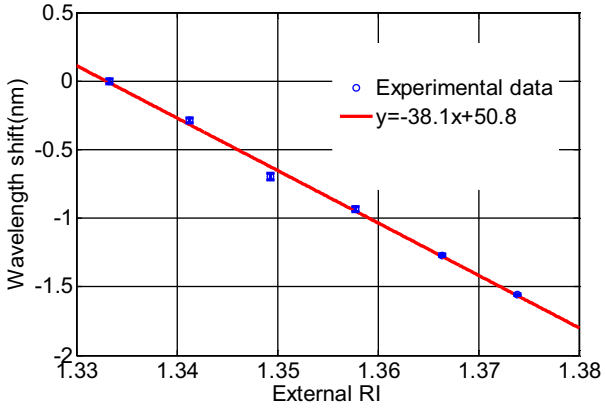

Fig. 6. Linear fitting and error bars of the relationship between external RI and wavelength shift.

tively stand for the amplitude noise, thermal variation of the system and the spectral resolution of the system setup. It is found that within the ranges of parameters considered here, the standard deviation of the resulting spectral variation can be approximated by:

$$\sigma_{ampl-noise} \approx (FWHM)/(4.5 \times (SNR)^{0.25}) \quad (2)$$

where SNR is complex to be measured in spectrum so it is assumed around 60 dB in such a spectrum with good quality as reference [18]. The FWHMs of the interference spectrum and laser spectrum in experiments are approximately 5.33 nm and 0.016 nm. Therefore, the standard deviations of both resulting spectral variation calculated by Eq. (2) are 0.037 and 1.12×10^{-4}. Here, the typical convention of establishing the resolution as 3 σ of the noise in the system is used as:

$$R = 3\sigma = 3\sqrt{\sigma^2_{ampl-noise} + \sigma^2_{temp-induced} + \sigma^2_{spect-tes}} \quad (3)$$

The temperature stabilization of$\sigma_{temp-induced}$ is 10 fm, which is generally small enough to be ignored. The resulting error due to spectral limitations of the detection device can be modeled as quantization error. There is a calculation as$\sigma_{spect-res} = R_w/2\sqrt{3}$ in which the R_w is the wavelength scanning resolution of the OSA. To give a guarantee to the spectral quality, $R_w$is set to be 0.2 nm and 0.02 nm for the interference spectrum and laser spectrum in Fig. 4. According to Eqs. (1)–(3), the calculated sensor resolutions before and after combining with the EDF ring cavity laser are 0.21 nm and 0.017 nm respectively. Although the sensitivity is almost equal, the DL is improved more than 10 times. It should be pointed that there is a trade-off between the SNR and scanning resolution. Sometimes, the spectral quality is not so satisfactory because too much noise disturbs the measurement. In other words, the resolution of the spectrum doesn't deserve the high scanning resolution. However, turning down the scanning resolution to match the resolution of the spectrum is a less-than-ideal alternative and cannot ensure the high sensor resolution.

3. Experiments and results

To verify the contribution of the proposed work, two parameters of liquid RI and ambient temperature are tested. When the environmental parameters change, the sensitivity of spectrum response can be expressed as:

$$S = \frac{\partial\lambda}{\partial E} = \frac{\lambda}{\Delta n_{eff}}\left(\frac{\partial n^{co}_{eff}}{\partial E} - \frac{\partial n^{cl}_{eff}}{\partial E}\right) + \frac{\lambda}{L}\frac{\partial L}{\partial E} \quad (4)$$

where E stands for ambient temperature or external RI value. Δn_{eff} is the difference between n^{co}_{eff} and n^{cl}_{eff}, which are respectively the effective refractive indices of core and cladding modes. Because of the generation of evanescent wave on the interface between external media and silica fiber cladding, n^{cl}_{eff} would change with the variation of external RI. At the same time, n^{co}_{eff}as well as the length of interference arm L remain unchanged. So the items of $\frac{\partial n^{co}_{eff}}{\partial E}$ and $\frac{\partial L}{\partial E}$ are equal to 0.

According to Eq. (4), the blue shift would happen in interference spectrum when the surrounding RI increases, which is consistent with the experimental results shown in Fig. 5. In experiment, the sensor setup has been shown in Fig. 3. NaCl solutions with different RIs are prepared as analytes. The MZ interferometer is fixed by a pair of three-dimension moving stages with a height adjustable flat under it. The sensing part is immersed by different RI solutions and the moving spectra are detected by an OSA. For each point in Fig. 6, the adjustable flat goes down to remove the liquid and then the sensing part is rushed slightly by distilled water. Fig. 6 shows the fitting curve between liquid RI and wavelength shift with error bars. And the sensitivity of −38.1 nm/RIU is obtained.

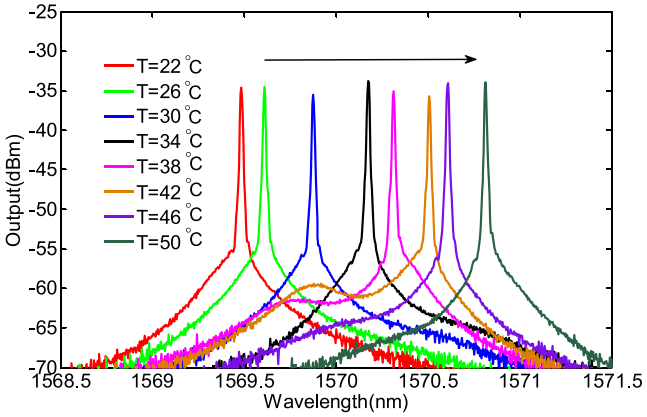

Fig. 7. Measured emission laser lines shifted along ambient temperature.

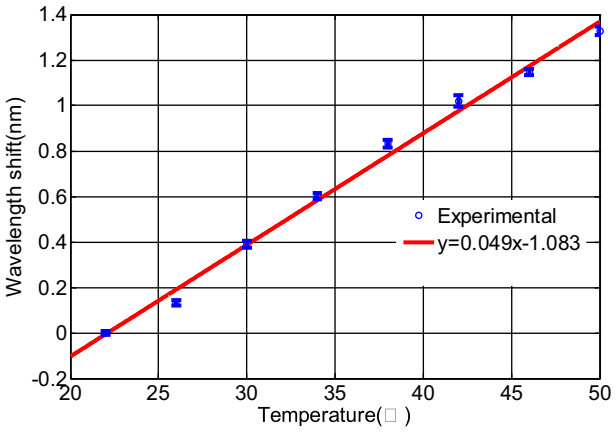

Fig. 8. Linear fitting and error bars of the relationship between temperature and wavelength shift.

The DL of RI measurement for the laser sensor is calculated as 4.54×10^{-4}. The maximum measurement error for RI sensing is given as $\pm 3.21 \times 10^{-4}$. In the recording process, the wavelength scanning resolution of OSA is set to be 0.02 nm.

The temperature characteristic is also investigated in experiment. The temperature variation leads to the change of fiber length and fiber RI through the thermal expansion effect and thermo-optic effect. So the interference length L and modal effective RI in Eq. (4) would be changed as a consequence. Assuming E is the temperature, the items of $\frac{\partial n_{eff}^{co}}{\partial E}$ and $\frac{\partial n_{eff}^{cl}}{\partial E}$ are the thermo-optic coefficients (TOCs) of the fiber core and cladding. The magnitude of silica material's TOC is around 10^{-6}, and the TOC of fiber core is slightly higher than that of cladding. $\frac{\partial L}{\partial E}$ is the thermal expansion coefficient (TEC) and its value is around 10^{-7}. Thus, the temperature sensitivity is positive and the value is around dozens of picometer per degree centigrade. It is consistent with the experimental result.

In experiment, the sensing setup shown in Fig. 3 is also applied to temperature measurement. The MZ interferometer is fixed by a pair of three-dimension moving stages and it is immersed in a hot water bath whose temperature is measured by a thermoelectric thermometer. So the temperature of the sensing part is changed steadily with a cooling process. The measured temperature range is from 22 °C to 50 °C. The moving single laser line is shown in Fig. 7. It can be seen that with the increase of temperature, there is a red-shift performance keeping pace with Eq. (4). And the relationship between temperature and wavelength shift with error bars is fitted as Fig. 8. The sensitivity and DL of temperature measurement for the laser sensor are calculated to be 0.049 nm/ °C and 0.35 °C. The maximum measurement error for temperature sensing is given as ±0.28 °C, respectively. The laser spectrum possesses high SNR and narrow FWHM, as well as gives a good capability in DL.

In addition, the spectral quality factor Q value is also calculated using the formula presented in reference [20]. The product of sensitivity S, $S/FWHM$, and visibility V can be used to express the Q value:

$$Q = K \cdot S^2/FWHM \cdot V \tag{5}$$

where the K is a unit coefficient to normalize the physical dimension. The Q value which is just a constant without dimension is used to describe the comprehensive sensing quality, including the sensing sensitivity, resolution and accuracy. After calculating, the Q values for the RI measurement and temperature are respectively 2.7×10^6 and 4.5. In order to clearly reveal the superiority in the sensing capability, a comparison is listed in Table 1. The DLs, Q values of these in-fiber MZ sensors are given and it can be seen that the DL of the laser sensor proposed in this paper is much higher than that of the simple cascaded core-offset structure [10], as well as higher than that of the modified sensing structure with fiber taper and thin core fiber (TCF) et al. like [11–14]. Remarkable Q values about two orders of magnitude higher than that in the aforementioned references are obtained.

It should be noted that the lateral core-offset distance in this paper is just about 3.7 μm which is shorter than other reports in the table. This laser sensor tactfully achieves high DL providing avoiding the increase of the fabrication difficulty and frangibility. As the SNR cannot be calculated in spectrum at once, the SNRs of these sensors giving in Table 1 are all considered as good as 60 dB even

Table 1
Comparison between references based on core-offset structure and the sensor in this paper.

structure		[10] Two core-offset joints	[11] Two core-offset joints + thinned taper joint	[12] Core-offset joint + up-taper joint	[13] Core-offset joint + MMF segment	[14] Core-offset joint based on TCF	This paper Two core-offset joints
Offset distance (μm)		~7	~5	~6.5	~4	~10	~3.7
ER(dB)		8	15	15	17	18	30
FWHM(nm)		5	0.75	2.4	1.16	0.73	0.016
R_w(nm)		0.01	0.015	0.02	~0.02	~0.02	0.02
R(nm)		0.11	0.02	0.053	0.030	0.023	0.017
S	RI(nm/RIU)	−33.3	−43.7	–	−64.89	–	−38.10
	T (nm/°C)	–	–	0.068	0.073	0.051	0.049
Q	RI	1.77×10^3	3.70×10^4	–	6.17×10^4	–	2.72×10^6
	T	–	–	0.03	0.08	0.06	4.5
DL	RI	3.18×10^{-3}	4.68×10^{-4}	–	4.62×10^{-4}	–	4.54×10^{-4}
	T	–	–	0.79	0.41	0.45	0.35

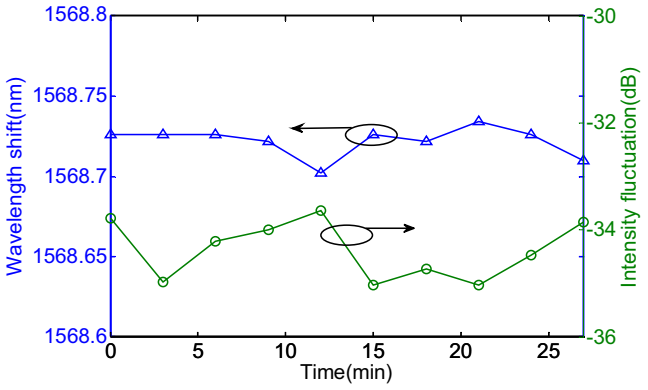

Fig. 9. Change of central wavelength and peak intensity in stability test.

if the spectral noise in some references is obviously much higher than that of this paper.

Finally, the stability of the MZ based EDF cavity laser sensor is tested. Laser line is scanned repeatedly for 10times with a time interval of 3 min, and the central wavelength and peak intensity are all recorded as shown in Fig. 9. The ambient temperature is room temperature kept in 20 °C. Obviously, the laser spectrum of this EDF cavity fiber laser sensor almost remains unchanged. The maximum changes of the central wavelength and peak intensity are 0.028 nm and 1.382 dB, respectively. Since the wavelength shift is comparable with the highest scanning resolution of the OSA (0.02 nm), the disturbance can be hardly distinguished by this EDF cavity laser sensor.

It should be pointed out that the calculated DL and sensor resolution as Eqs. (1)–(3) expressed can reflect the sensing capability of the sensor itself to some degree. In this paper, only the theoretical value is given for which the sensor has the ability to achieve. When it comes to the stability, there are so many factors to decide it. The detection limit is indeed affected by the stability of the sensor, which is relative to the factors like RI of NaCl, the measurements made by the OSA, temperature fluctuations and so on. It is expected that these problems could be solved in the future by good package and algorithm. Here, only a sensing method is provided with potential application. Regarding to the power change, it is introduced by the vibration-sensitive system including EDF ring cavity and core-offset structure while it doesn't affect the measurement results, and it can be further alleviated via good package.

4. Conclusion

In this paper, an EDF ring cavity laser sensor for RI and temperature is investigated. A core-offset MZ interferometer is inserted into the fiber ring cavity laser as a tunable filter. The experiments prove that the spectral quality factor Q is increased significantly. Furthermore, the sensor resolution and DL are also improved through this fiber ring cavity laser device. The DLs of this laser sensor for RI and temperature measurement are respectively 4.54×10^{-4} and 0.35 °C. For the core-offset structure, it is an efficient way to improve the sensing capability instead of controlling offset distance and direction. The proposed sensor is cost-effective, easy being fabricated and has the advantages of low cost, simple operation and easy fabrication process.

Acknowledgements

This work was supported in part by the National Natural Science Foundation of China under Grant 61425003, the Fundamental Research Funds for the Central Universities under Grant N140404021, N150401001, and State Key Laboratory of Synthetical Automation for Process Industries under Grant 2013ZCX09.

References

[1] L. Xueming, Y. Xiufeng, L. Fuyun, et al., Stable and uniform dual-wavelength erbium-doped fiber laser based on fiber Bragg gratings and photonic crystal fiber, Opt. Express 13 (1) (2005) 142–147.
[2] W.L. Yong, B. Lee, Wavelength-switchable erbium-doped fiber ring laser using spectral polarization-dependent loss element, IEEE Photonics Technol. Lett. 15 (6) (2003) 795–797.
[3] Z. Fu, D. Yang, W. Ye, et al., Widely tunable compact erbium-doped fiber ring laser for fiber-optic sensing applications, Opt. Laser Technol. 41 (4) (2009) 392–396, Journal of Lightwave Technology, 2012, 30 (23): 3569–3575.
[4] H. Young-Geun, L. Sang, K. Chang-Seok, et al., Simultaneous measurement of temperature and strain using dual long-period fiber gratings with controlled temperature and strain sensitivities, Opt. Express 11 (5) (2003) 476–481.
[5] Q. Wang, Z. Ma, Feedback-stabilized interrogation technique for optical Fabry–Perot acoustic sensor using a tunable fiber laser, Opt. Laser Technol. 51 (51) (2013) 43–46.
[6] M. Gonzalez-Reyna, E. Alvarado-Mendez, J.M. Estudillo-Ayala, et al., Laser temperature sensor based on a fiber bragg grating, IEEE Photonics Technol. Lett. 27 (11) (2015) 1141–1144.
[7] X. Lan, J. Huang, Q. Han, et al., Fiber ring laser interrogated zeolite-coated singlemode-multimode-singlemode structure for trace chemical detection, Opt. Lett. 37 (11) (2012) 1998–2000.
[8] Zhi-bo Liu, Zhongwei Tan, Bin Yin, Yunlong Bai, Shuisheng Jian, Refractive index sensing characterization of a singlemode–claddingless–singlemode fiber structure based fiber ring cavity laser, Opt. Express 37 (11) (2012) 5037–5042.
[9] Z.B. Liu, B. Yin, X. Liang, et al., Axial strain and temperature sensing characteristics of the single–coreless–single mode fiber structure-based fiber ring laser, Appl. Phys. B 117 (2) (2014) 571–575.
[10] Z. Tian, S.H. Yam, In-line single-mode optical fiber interferometric refractive index sensors, J. Lightwave Technol. 27 (13) (2009) 2296–2306.
[11] S. Jie, X. Shilin, Y. Lilin, et al., A sensitivity-enhanced refractive index sensor using a single-mode thin-core fiber incorporating an abrupt taper, Sensors 12 (4) (2012) 4697–4705.
[12] Z. Shanshan, Z. Weigang, G. Shecheng, et al., Fiber-optic bending vector sensor based on Mach-Zehnder interferometer exploiting lateral-offset and up-taper, Opt. Lett. 37 (21) (2012) 4480–4482.
[13] J. Fan, J. Zhang, P. Lu, et al., A single-mode fiber sensor based on core-offset inter-modal interferometer, Opt. Commun. 320 (2) (2014) 33–37.
[14] Z. Jiangtao, L. Changrui, W. Yiping, et al., Simultaneous measurement of strain and temperature by employing fiber Mach-Zehnder interferometer, Opt. Express 22 (2) (2014) 1680–1686.
[15] Y. Zhao, X. Li, L. Cai, A highly sensitive Mach-Zehnder interferometric refractive index sensor based on core-offset single mode fiber, Sens. Actuators A: Phys. 223 (2015) 119–124.
[16] J. Chen, J. Zhou, Q. Zhang, et al., All-fiber modal interferometer based on a joint-taper-joint fiber structure for refractive index sensing with high sensitivity, Sens. J. IEEE 13 (7) (2013) 2780–2785.
[17] D.W. Duan, Y.J. Rao, L.C. Xu, et al., In-fiber Mach–Zehnder interferometer formed by large lateral offset fusion splicing for gases refractive index measurement with high sensitivity, Sens. Actuators B Chem. 160 (1) (2011) 1198–1202.
[18] I.M. White, F. Xudong, On the performance quantification of resonant refractive index sensors, Opt. Express 16 (2) (2008) 1020–1028.
[19] Z. Tian, S.S.H. Yam, Loock H P: single-Mode fiber refractive index sensor based on core-offset Attenuators, Photonics Technol. Lett. IEEE 20 (16) (2008) 1387–1389.
[20] X. Bai, D. Fan, S. Wang, et al., Strain sensor based on fiber ring cavity laser with photonic crystal fiber in-line Mach–Zehnder interferometer, IEEE Photonics J. 6 (4) (2014) 1–8.

Biographies

Lu Cai was born in Liaoning, China, in Jul. 1990. She received her B.A. degrees in the College of Information Science and Engineering from the Northeastern University, China, respectively in 2013. She is now a PhD student of Northeastern University. Her research interests are fiber optical sensors, modal interference sensors, in-fiber interferometer and its sensing applications. She has authored and co-authored several scientific papers.

Yong Zhao received his M.A. and Ph.D. degrees, respectively, in precision instrument & automatic measurement with laser and fiber-optic techniques from the Harbin Institute of Technology, China, in 1998 and 2001. He was awarded a first prize scholarship in 2000 by the China Instrument and Control Society and the Sintered Metal Corporation (SMC) scholarship in Japan. He was a scholarship in Japan. He was a postdoctor in the Department of Electronic Engineering of Tsinghua University from 2001 to 2003, and then worked as an associate professor in the Department of Automation, Tsinghua University of China. In 2006, he was a visiting scholar of University of Illinois in Urbana and Champagne, USA. In 2008, he was awarded as the New Century Excellent Talents in University by the Ministry of Education of China. In 2009, he was awarded as the Liaoning Bai-Qian-Wan Talents by Liaoning Province. In 2011, he was awarded by the Royal Academy of Engineering as an academic researcher of City University London. He was awarded by the National Science Foundation for Distinguished Young Scholars of China, in 2014. Now he is working in Northeastern University as a full professor. As a leader of his research group, his current research interests are the development of fiber-optic sensors and device, fiber Bragg grating sensors, novel sensor materials and principles, slow light and sensor technology, optical measurement technologies. He has authored and co-authored more than 200 scientific papers and conference presentations, 10 patents, and 4 books. He is a member in the Editorial Boards of the international journals of Sensor Letters, Instrumentation Science & Technology, Journal of Sensor Technology, and Advances in Optical Technologies.

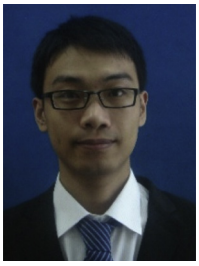

Xue-gang Li was born in Hebei, China, in December 1991. He received her B.A. degrees in the College of Information Science and Engineering from the Northeastern University, China, respectively in 2014. He is now a PhD student of Northeastern University. He research interests are fiber optical sensors, modal interference sensors, in-fiber interferometer and its sensing applications. He has authored and co-authored several scientific papers.